COVER PAGE

Document downloaded by @DAEL

Sat Nov 28 14:39:03 2026
For personal use

When automatic English translation is provided, only the original document is authentic.
The EAA cannot be held responsible of any translation error

Bibliographical reference

Model Calculations With a Fast Field Programme and Comparison With Selected Procedures to Calculate Road Traffic Noise Propagation Under Defined Meteorological Conditions, Rainer Matuschek, Volker Mellert and Stylianos Kephalopoulos, Acta Acustica **vol. 95** (Number 5), 2009, pp. 941-949

DOI
https://doi.org/10.3813/AAA.918224

ACTA ACUSTICA UNITED WITH ACUSTICA
Vol. 95 (2009) 941 – 949

DOI 10.3813/AAA.918224

Model Calculations With a Fast Field Programme and Comparison With Selected Procedures to Calculate Road Traffic Noise Propagation Under Defined Meteorological Conditions

Rainer Matuschek*, Volker Mellert
Oldenburg University, Institute for Physics, 26111 Oldenburg, Germany.
matuschek@itap.de, volker.mellert@uni-oldenburg.de

Stylianos Kephalopoulos
JRC, Institute for Health and Consumer Protection, 21020 Ispra, Italy

Summary
National guidelines for calculating noise propagation are still in use though progress was made to develop a unified scheme for sound propagation outdoors by taking more physical parameters of the propagation path into account. Besides comprehensive models simpler and faster calculations are under development in order to be used as an engineering model. Widespread classical engineering models from different European countries are compared in this study with physical wave propagation from a defined line source representing traffic noise. The numerical model is based on a fast-field programme. This scheme allows for a very fast calculation of wave propagation in a layered medium including complex boundary conditions. Source properties are carefully adjusted for comparison and the respective meteorological conditions of national guidelines are taken into account. It turns out that the different guidelines are in good agreement with exact calculations up to distances about 1000 m. The so-called downwind condition gives an excellent estimate for the conditions most favourable for sound propagation. The fast numerical calculation scheme enables easy systematic variation of e.g. source properties, meteorological conditions and ground impedances for any sensitivity analysis.
PACS no. 43.28.Fp, 43.50.Vt

1. Introduction

The environmental noise directive 2002/49/EC triggered the initiative of European acousticians to investigate noise mapping procedures in order to incorporate more detailed knowledge of the physics of sound propagation outdoors into existing calculation schemes and finally to unify the different approaches of national guidelines to a general "European model". Two research projects have been funded by the European Commission: "HARMONOISE" (2001- 2004) and "Imagine" (2004-2006) [1]. Results of these investigations are recently published in a special session of Acta Acustica united with Acustica [Vol. 93(2), (2007)]. One of the leading scientists of these projects, Eric Salomons, introduces the main results of this special issue with an excellent overview in the preface [2].

An important influence on sound propagation is given by the vertical sound speed profile in the atmosphere, which is determined by the meteorological conditions. Substantial improvements have been achieved in characterising the atmospheric boundary layer with respect to sound propagation [3]. From long-term experience it is well known that certain meteorology is supportive for sound propagation. Based on this knowledge, existing engineering models for calculation noise propagation take the "worst case condition" into account by appropriate general rules (e.g. "downwind" condition). It is not very clear, if the different rules in still existing or transitional arrangement in national guidelines reflect a comparable class of meteorological conditions. Though the new development by HARMONOISE aims at a comprehensive model of propagation with identifiable physical parameters of impact [4] the 25 classes of meteorological conditions might be too sophisticated from the point of view of long-term experienced engineering models. An additional attempt to calculate sound propagation by combining physical models and heuristic experience is developed in HARMONOISE [5]. The aim of the present paper is to evaluate existing prediction schemes in order to quantify the validity of these or for the respective propagation condition, and to provide supplementary information for temporary regulations, which are recommended and in use until a unified European guideline comes into force.

Received 3 January 2008,
accepted 27 May 2009.

* now: itap GmbH, Marie-Curie-Str. 8, 26129 Oldenburg, Germany

© S. Hirzel Verlag · EAA

The most important existing European guidelines are compared in this paper with a numerical prediction scheme based on wave propagation in layered media. The guidelines and protocols are not easy to compare. The reasons lie in the different assumptions of source spectrum, power and geometry, on different propagation channels with different meteorological, geometrical and impedance statements. The investigation is therefore restricted to traffic noise with a line source of certain vehicle density, sound power level and a general assumption on the traffic noise spectrum. Source and receiver height are adjusted between the different prediction schemes after close inspection of guideline details. The input is thus chosen according to the respective guideline in the sense of source geometry, source strength, spectral distribution and directivity.

The noise propagation is calculated for various assumptions on ground impedance and meteorology, in case these parameters are taken into account in the existing prediction schemes. The calculations according to existing guidelines are performed with two commercial software packages [6, 7].

The results of the guideline calculations are compared with a numerical wave propagation scheme (FFP) which is able to take (stratified) meteorological conditions and ground impedance into account. According to [8] the FFP was not used for the development of a reference model in HARMONOISE. The numerical scheme enables investigation of variation in the meteorological conditions and the ground impedance systematically. The underlying conditions of the propagation channel of the guidelines are indirectly identified by this approach and the range of validity confirmed.

Furthermore, it is possible to define benchmark cases of meteorology and ground impedance, and to quantify the influence on traffic noise propagation.

2. Description of the Fast Field Programme (FFP) for noise propagation modelling

The Fast Field Programme [9] [10] used was written by the acoustics group of Keith Attenborough (Open University, Milton Keynes, UK) and has been used for a number of outdoor propagation problems and by our group mainly for underwater wave propagation prediction. We are unaware of any publication on FFP basis dealing with the prediction of the sound field of line sources such as roads or railway tracks.

In short the sound propagation from a point source in a layered atmosphere or ocean can be dealt with by first Fourier-transforming the time-dependent wave equation with respect to time which leads to the Helmholtz-equation. Because of the horizontal stratification of the medium a separation in cylindrical coordinates can be performed leading to the so called depth-separated wave equation. The range-dependent part of the wave is then transformed to k-space by means of a Hankel transform. If the acoustic properties inside each layer are constant, the Green's function can be calculated that obeys the boundary conditions between adjacent layers. Inside the topmost and bottommost layers the Sommerfeld radiation condition replaces the missing boundary conditions since there is only one layer adjacent. This calculation has to be repeated for each receiver height z where one wants to know the resulting wave field. An inverse Hankel-transform of the Green's function followed by a multiplication with the z-dependent part of the wave solution finally yields the wave field in (r, z) space. Since the inverse Hankel-transform for complex arguments is a computationally rather time consuming task that can be approximated by a simple Fast-Fourier-transform when the argument fulfills $kr \gg 1$, the method is called Fast-Field-Algorithm. It should be noted that the FFP used is for axisymmetric problems (2-dimensional), so that the effect of varying wind speed and direction enters in form of an effective sound speed.

An important feature of the FFP is its computational speed which allows to calculate different realizations of the frozen atmosphere in real time. In its present form the FFP can not cope with inhomogenous propagation conditions in the direction of sound propagation, i.e. topography, range-dependent ground impedance or atmospheric turbulence. The last however could be modelled as a stochastic fluctuation of the vertical stratification of the atmosphere and as such be computed as an ensemble average over suitable realizations of the atmospheric state, as proposed by Chevret *et al.* [11]. An analytically-based method for including turbulence in FFP was proposed in [12]. Coupling of range-dependent topography and atmospheric conditions with a parabolic equation model of less computational speed was recently accomplished by [13].

In order to make sure that the prediction software is used correctly some pre-tests were carried out with the same parameters as in [14] test cases No. 1 and 2. These benchmark cases describe the problem of a point source above an (acoustically) medium hard ground for a constant (case 1) and linearly increasing (case 2) sound speed profile. The implementation of the FFP used in the present paper provides practically the same results, if an appropriate discretisation of the sound speed gradient and the correct atmospheric condition for absorption are taken into account: A comparison of the transmission shows very good agreement of the solutions for the three frequencies 10 Hz, 100 Hz and 1 kHz within an error range just noticeable, if at all, in the graphical presentation.

The ground impedance model used in the calculations is a Biot/Attenborough model for rigid poroeleastic semi-infinite ground. The ground is modelled as a poroelastic layer of 2 m depth above a nonporous substrate. The parameters describing these two layers are exactly as given in Table 1 in [14]. Only the flow resistivity was chosen to be variable and its value is given with the corresponding calculations.

2.1. Field of a point source above rigid ground and above a ground with realistic impedance

Two simulations serve to isolate the influence of ground flow resistivity on the resulting sound field (Figure 1). In

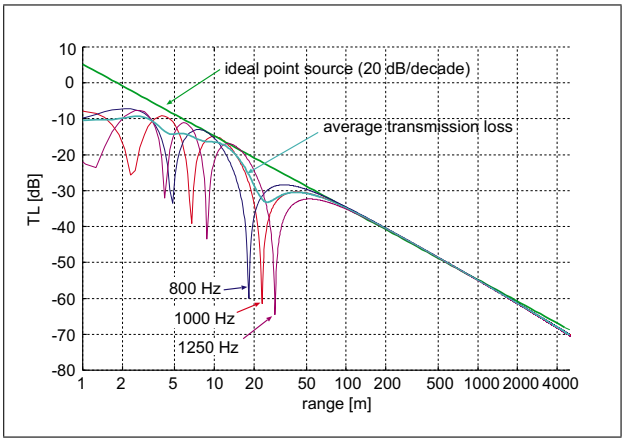

Figure 1. Transmission loss (TL) of a point source above hard ($\sigma = 3.66 \cdot 10^{12}$ Pa s/m^2) ground as a function of distance. The three curves with strong interference minima are computed for frequencies of 800, 1000 and 1250 Hz from left to right (at the interference minimum) respectively. Also shown is the average TL in the 1/3 octave-band calculated for the three discrete frequencies given as well as the TL for an ideal point source above a hard ground with its characteristic decay of 20 dB/decade.

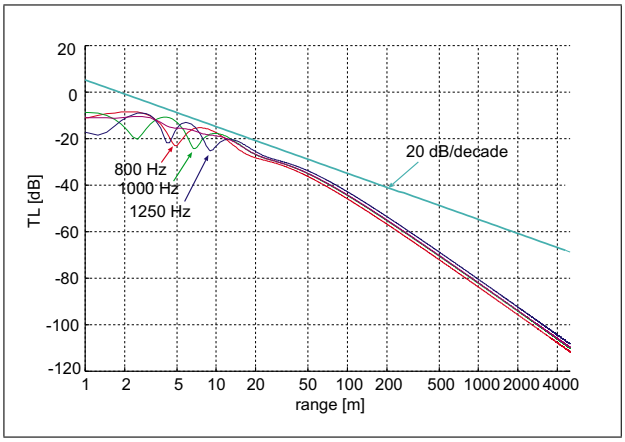

Figure 2. TL of a point source above normal ground ($\sigma = 2.5 \cdot 10^5$ Pa s/m^2) as a function of distance. The three curves for 800, 1000 and 1250 Hz (from bottom to top) as well as the averaged TL curve that is nearly identical to the 1 kHz curve do not exhibit interference minima for ranges exceeding 20 m. The decay is about 38 dB/decade.

the first case a nearly rigid bottom with a flow resistivity of $3.66{\cdot}10^{12}$ Pa s/m^2 is investigated. The sound speed of 343 m/s is taken to be constant with height. Source and receiver heights are 0.5 m and 4 m respectively as proposed e.g. in the German RLS-90 guideline. Figure 1 shows the transmission loss as a function of range for this point source for the three 1/3-octave band center frequencies of 800, 1000 and 1250 Hz.

The result for very short ranges less than about 5 m is not to be taken too seriously because of the discretization of Δr and the FFP inherent condition $kr \gg 1$. This however does not influence the result for larger ranges.

The curves clearly show sharply pronounced interference dips up to a range of ca. 30 m where the interference produces losses of up to 40 dB. Also shown is the average TL computed from the three single frequency cases by incoherent summation. This curve of course shows a much smoother appearance resulting in maximum deviation of only about 10 dB at the dip. The straight green line has a slope of -6 dB/range doubling. All computed TL curves show this characteristic slope of geometrical point source attenuation for ranges greater than about 100 m. The effect of atmospheric absorption has not been taken into account for these simulations since they are meant to show the effect of ground impedance on the slope of the TL curves.

The simulation for this nearly rigid bottom implicates that in order to model sound sources that occupy a larger area such as e.g. a road one has to average over neighbouring frequencies to get rid of the interference. For natural grounds such as grassland however, the lower flow resistivity leads to a smaller ground impedance and hence less pronounced destructive interference effects. This is demonstrated in Figure 2 where the ground is modelled with a flow resistivity of $2.5{\cdot}10^5$ Pa s/m^2.

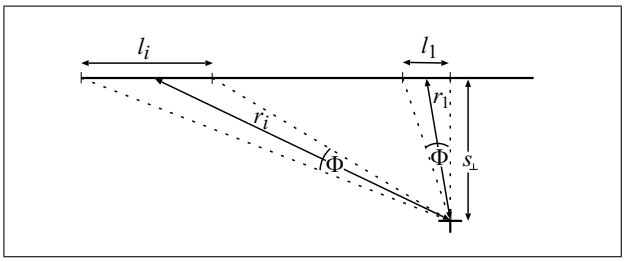

Figure 3. Sketch of road segmentation. The view angle Φ is kept constant for each segment of the road which leads to successively larger segment lengths l_i. r_i designates the distance to the ith corresponding point source.

This figure shows two effects of a porous ground on the sound transmission. Firstly the interference dips nearly vanish leading to a monotonous decrease of TL with range. Secondly the slope of the TL curves become steeper, in this case they decrease by about -38 dB/range–decade.

The average TL is nearly indistinguishable from the 1 kHz TL curve at distances exceeding 20 m. This implies that it should be feasable to model an incoherent line source like a traffic road or a railroad track by a number of linearly arranged point sources.

2.2. Description of the algorithm to compute line source generated sound fields

The road is modelled as a number of incoherent point sources with source strength proportional to the number of passing cars per time and to the length of the road segment. The location of each point source is given by the vector r_i from the receiver to the middle of the i-th segment with length l_i as sketched in Figure 3.

The sections l_i of this straight long road are computed under the constraint of a constant view angle Θ of 5° as seen from the receiver location (point of sound immission) for every section. This yields relatively short sections

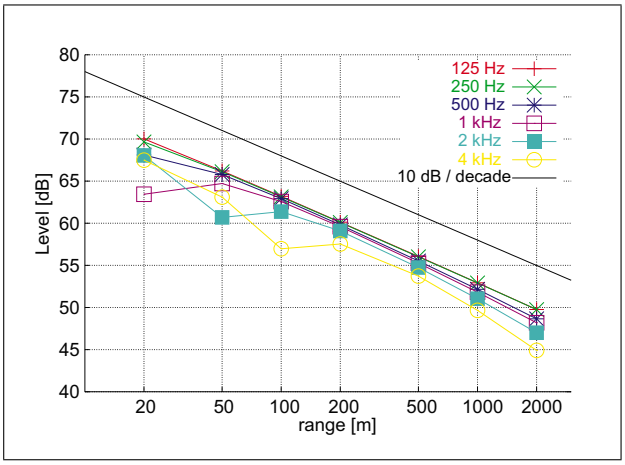

Figure 4. Sound pressure levels for a simulated line source, consisting of point sources located at each of the road segments with a view angle of 5°. Calculations are shown for the six octave band center frequencies 125, 250, 500, 1k, 2k and 4 kHz.The ground is modelled as acoustically hard with a flow resistivity $\sigma = 2.5 \cdot 10^{10}$ Pa s/m^2. The TL curves slopes show the expected −10 dB/decade decay characteristic for a line source. Pure-tone interference is visible for higher frequencies below distances of 200 m. The interference will be smoothed out in later calculations according to the procedure outlined in 2.3.

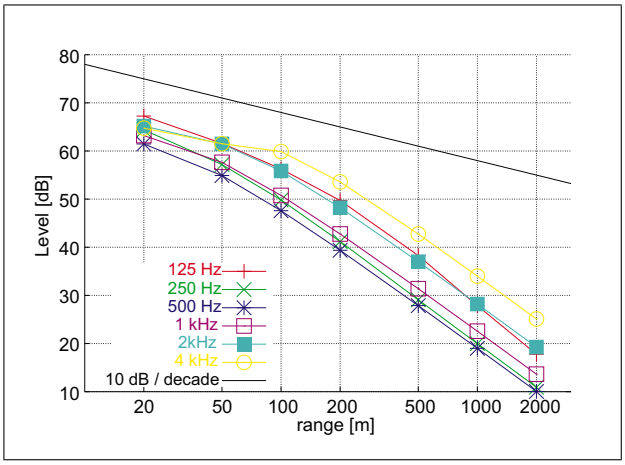

Figure 5. Sound pressure levels for a simulated line source as in Figure 4 but for a transmission above ground with a more realistic flow resistivity of $\sigma = 2.5 \cdot 10^5$ Pa s/m^2 such as grass land. The slope of the TL curves is about −28 dB/decade.

of l_1 =1.75 m length for 20 m distance ($s_\perp$) between the road and the receiver. The last section of the road has a length of 115.18 m for this case. Since the distance from the middle of the respective section to the receiver also varies (from 20.02 m to 172.18 m for this particular example), one cannot simply neglect the influence of those parts of the road that are farther away. For free field propagation and neglecting atmospheric absorption every segment contributes the same to the total sound power received. For a typical grass land with a flow resistivity of $2.5 \cdot 10^5$ Pa s/m^2 the sound level difference between the nearest and the farmost section for this example is about ½ dB when neglecting atmospheric absorption.

Since the influence of a wind velocity profile on sound propagation will only be investigated for the two extremes of downwind and upwind conditions, the problem is symmetric and only one half of the road needs to be sectioned for the computations.

Strictly speaking the 2-dimensional FFP algorithm can not be used for the simulation of sound propagation in the atmosphere which can be modelled as a moving layered medium. That is because in moving media the wave fronts are no longer perpendicular to the propagation direction of the sound field. For small angles however it can be shown that the difference can be neglected [15]. Traffic noise sources are typically directly above the ground (50 cm) where the wind velocity is small. A similar argument holds true for the receiver (3–4 m above the ground). Therefore the use of an effective sound speed c_{eff} as the sum of the adiabatic sound speed and the projection of the horizontal wind velocity on the direction from source to receiver can be justified.

Figures 4 and 5 show the resulting transmission loss for road traffic noise as a function of range. The computations were performed for the six octave band center frequencies of 125, 250, 500, 1k, 2k and 4k Hz, where some of the European guidelines give sound power levels for traffic noise.

In case of a nearly rigid bottom between source and receiver there are some interference effects visible in the TL curves for 1k, 2k and 4 kHz. For the grass land simulation in Figure 5 these effects vanish as in the case of point source propagation. The slope of the TL curve for this simulated line source above rigid ground is about −10 dB/decade as to be expected for cylindrical spreading.

2.3. The traffic noise spectrum

Some of the European guidelines on traffic noise prediction suggest the computation of noise immission in octave or 1/3 octave bands, thus some kind of reference source spectrum is needed. The French *NMPB-Route* uses the octave spectrum given in the *Guide du Bruit*. The austrian *RVS-3.02* proposes a similar spectrum and finally the European *EN-1793-3* contains a 1/3-octave spectrum that is to be used for evaluation of noise barrier efficiency. While the French spectrum is normalized to a total of 70 dB(A), the other two give the levels re 0 dB(A) total. All spectra given are A-weighted and shown in Figure 6.

The HARMONOISE/IMAGINE source model differentiates between rolling noise and propulsion noise with different source heights. To keep the computations as simple as possible and to ensure the comparison between different guidelines, we used the 1/3-octave spectrum given in EN-1793-3.

A last question concerning the simulation of road traffic noise by linearly arranged point sources concerns the number of frequencies per octave band that need to be averaged in order to obtain reliable results. As was shown in Figures 1 and 2 an acoustically hard bottom leads to deep interference dips in the propagation calculations for a monofrequency point source. An extended sound source such as

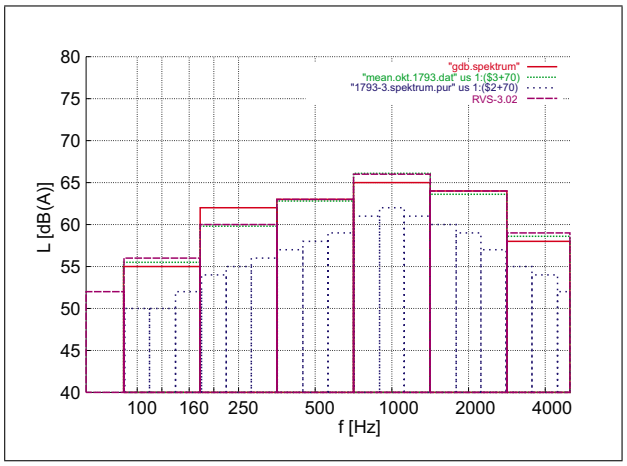

Figure 6. A-weighted octave spectra for traffic noise in 30 m distance from the road taken from the French guideline "Guide du Bruit" and 1/3-octave as well as the derived octave spectrum from the European guideline EN-1793-3. Since the 1/3-octave spectrum of EN-1793-3 is given re 0 dB(A) total, 70 dB were added to ease the comparison.

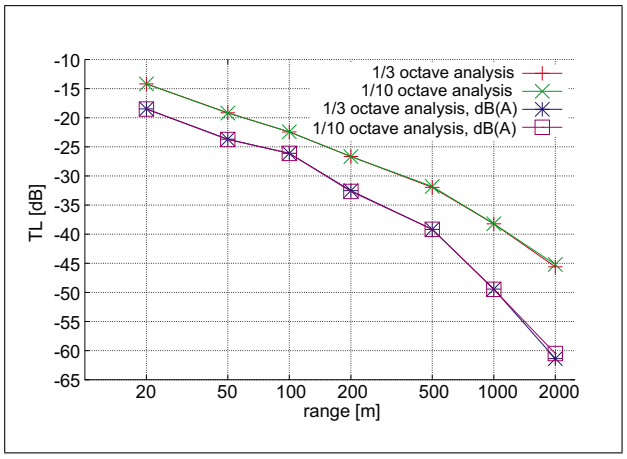

Figure 7. Comparison of transmission loss curves computed by averaging over 1/10 octave spaced frequencies with TL curves from 1/3-octave averaging. The lower two curves are derived by A-weighting the corresponding upper curve. The simulation was done for moderate downwind sound propagation and a stable atmospheric stratification.

a road segment surely will not produce those interference dips since especially for higher frequencies even the noise of a single car is not coherently emitted. To circumvent this problem in the simulation, the transmission loss for every road segment has to be computed for several frequencies in the respective octave band analyzed. Computations for 1/10 octave anaylysis in comparison with 1/3-octave analysis results are shown in Figure 7 for A-weighted and unweighted spectra.

The upper two curves show the unweighted transmission loss and are nearly indistinguishable. Only at the largest distance of 2 km they deviate slightly by about 0.5 dB. A-weighted transmission loss results have been derived from these curves by assuming a typical traffic noise spectrum as shown in Figure 6. As before a difference in the predicted transmission loss can only be seen at a perpendicular distance of 2 km between road and receiver. Both A-weighted curves show a difference of about 1 dB. Since the computing time per octave band is directly proportional to the number of frequencies used it was decided to accept this maximal error of 1 dB.

The time required to compute the transmission loss with only three frequencies per octave band for all of the 17 road segments and 10 atmospheric layers is about 2 hours on an AMD Athlon 1800 XP+.

3. Definition of the benchmark cases

3.1. Meteorological conditions

We use the Monin-Obhukov similarity theory in order to achieve realistic temperature and wind velocity profiles. Let the wind vector in cartesian coordinates be given as $(\overline{u} + u', \overline{v} + v', w')$ and the temperature as $\overline{T} + T'$, where the prime indicates the deviation from the respective mean value $(\overline{x})$. The mean vertical velocity component must be zero in a stratified atmosphere where the mean physical quantities are assumed to be functions of height only. The friction velocity $u_\star^2$ is a measure for transport of kinematic momentum flux and is defined as the covariance betweeen the horizontal and the vertical velocity components, i.e.

$$u_\star^2 = \sqrt{\overline{u'w'}^2 + \overline{v'w'}^2}, \tag{1}$$

$$T_\star = \frac{\overline{-w'T'}}{u_\star}. \tag{2}$$

$T_\star$ decribes the kinematic heat flux in the vertical direction and has a unit of temperature through normalization with the friction velocity. The Obukhov length L which characterizes the different atmospheric layerings is defined as

$$L = \frac{u_\star^2 \overline{T}}{\kappa g T_\star}, \tag{3}$$

with $g = 9.81\,\mathrm{m/s^2}$ the earth's acceleration, $\kappa = 0.41$ von Kármán constant and $\overline{T}$ the mean temperature of the boundary layer. The classification of the profiles by means of the Obukhov length is as follows:

$$\begin{aligned} -150\,\mathrm{m} < L < -1\,\mathrm{m}: &\quad \text{unstable atmosphere,} \\ 10\,\mathrm{m} < L < 200\,\mathrm{m}: &\quad \text{stable atmosphere.} \end{aligned}$$

As the the friction velocity is strictly positive, it can be seen that the difference between the unstable and the stable atmosphere is given by the sign of $T_\star$. A stable atmosphere is characterized by a positive temperature gradient $\mathrm{d}c/\mathrm{d}z$. A parcel of air that is moved adiabatically upward from some height z to $z + \Delta z$ will have a higher density then the surrounding air and thus will eventually fall down to its original height. The same holds true for a transport to a lesser height. To maintain this stable stratification the kinematic eddy heat flux, i.e. $T_\star$, has to be positive. This

Table I. Parameters for the different atmospheric profiles that have been prepared and used for the sound propagation benchmark calculations. The roman literals only serve to distinguish the different stable and neutral profiles and bear no relation to the classification of the german TA-Luft. Also given are the corresponding wind speed and stability classes according to the Harmonoise scheme, H-class.

profile	$u_\star$ [m/s]	$T_\star$ [°C]	L [m]	H-class.
stable	0.2	0.1	50.0	W2/S4
stable III	0.2	0.1	150.0	W2/S3–S4
neutral	0.1	0.001	500.0	W3/S3
neutral II	0.3	0.001	500.0	W2/S3
neutral III	0.2	0.001	500.0	W3/S3
neutral IV	0.25	0.001	500.0	W2/S3
unstable	0.3	-0.2	-50.0	W3/S2

situation is typical at night, when the ground cools due to radiation. At daytime the ground heats up faster than the air which leads to an unstable stratification.

In a neutral atmosphere the potential temperature is constant with height, so that the parcel of air from above can be positioned anywhere without exhibiting any restoring force. In terms of Obukhov length L and $T_\star$ this situation is given for $L > 200\,\mathrm{m}$ or $L < -150\,\mathrm{m}$ in combination with a positive but small temperature $0\,°\mathrm{C} < T_\star < 1\,°\mathrm{C}$.

It has to be noted, that for friction velocities less than about 0.05 m/s Monin-Obukhov theory can not be applied. The modulus of the length L can be interpreted as the height up to which the turbulence in the atmosphere is driven by wind shear.

$$u(z) = \frac{u_\star}{\kappa}\left[\ln\frac{z}{z_0} - \Psi_u\left(\frac{z}{L}\right)\right], \tag{4}$$

$$T(z) = \frac{T_\star}{\kappa}\left[\ln\frac{z}{z_0} - \Psi_T\left(\frac{z}{L}\right)\right] + T_0 + \Gamma z. \tag{5}$$

z_0 is called the roughness length that takes on values between 1 cm and 10 cm for grassland. Very flat terrain such as a water surface can have roughness lengths below 1 mm. $\Gamma = 0.01\,°\mathrm{C}$ is the adiabatic temperature factor.

For the scaling function Ψ_u and Ψ_T the Businger-Dyer relations as given by Stull [16] are used:

$L > 0$:

$$\Psi_u = 2\ln\frac{1+x}{2} + \ln\frac{1+x^2}{2} - 2\arctan x + \frac{\pi}{2},$$

$$\Psi_T = 2\ln\frac{1+y}{2},$$

$$x = \sqrt[4]{1-16\frac{z}{L}}, \quad y = \sqrt{1-16\frac{z}{L}};$$

$L < 0$:

$$\Psi_u = -5\frac{z}{L}, \qquad \Psi_T = -5\frac{z}{L}.$$

There are several free parameters in the governing equations (4) and (5) that are listed in Table I.

Propagation calculations are carried out for the four stability classes “very stable”, “stable”, “neutral” and “unstable” of the atmosphere. These classes are used for the

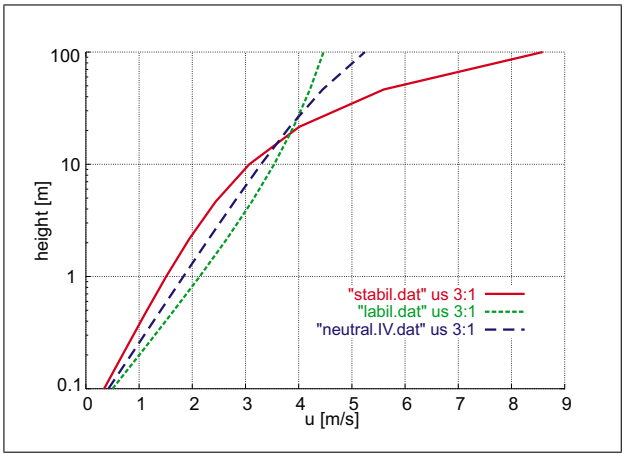

Figure 8. Typical wind speed profiles for stable, unstable and neutral atmospheric stratification. Note the logarithmic height scale in contrast to the following figures.

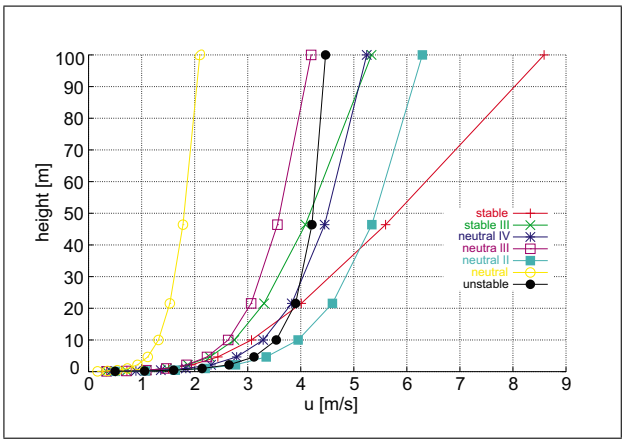

Figure 9. Wind velocity profiles for the modelled atmospheric states listed in Table I that were prepared for the sound propagation benchmark calculations.

the calculation of air pollution dispersion, and are the only differentiated weather conditions, which are defined in a present guideline (e.g. German TA-Luft). Appropriate classes for noise propagation have been worked out in the HARMONOISE project [4]. Their correspondence to the stability classes chosen is given in Table I.

All profiles are calculated for a temperature of $T_0 = 10°\mathrm{C}$, and a roughness length z_0 of 0.05 m. The stable atmospheric stratification describes an atmospheric state that leads to the so called *favourable propagation conditions for sound propagation* when applied for the downwind direction from sound source to receiver. Five meters above the ground the wind velocity should not exceed 3 m/s.

In comparison to the 25 wind and temperature profiles chosen in [3] it can be seen that all important stability classes for wind speeds less than 6 m/s are taken into account.

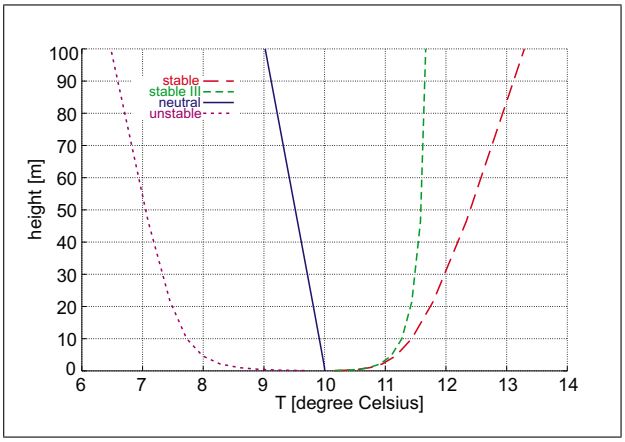

Figure 10. Corresponding temperature profiles of Table 1. Note that the different neutrally stable wind velocity profiles of Figure 9 all share the same temperature stratification.

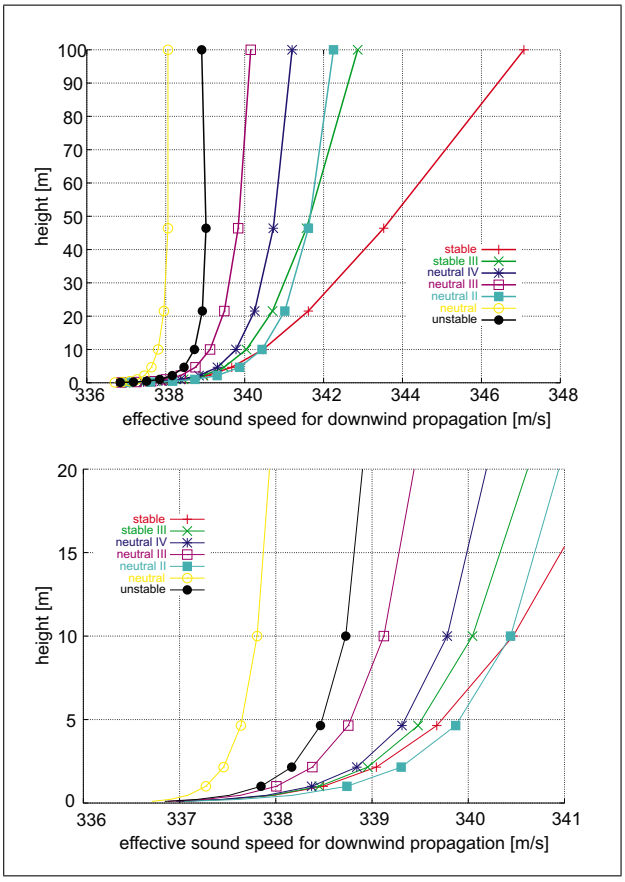

Figure 11. Effective sound speed for downwind propagation resulting from the combination of wind and temperature profiles for the different meteorological classes given in Table I. The bottom graph contains a zoomed in view of the sound speed profiles near the ground.

3.2. Comparison of FFP simulations with predictions according to the European guidelines

A comparison of the prediction of some of the European guidelines for a long straight road is shown in Figure 12. Computations were carried out for a traffic flow rate of 24000 passenger cars per 24 hours, i.e.an hourly traffic

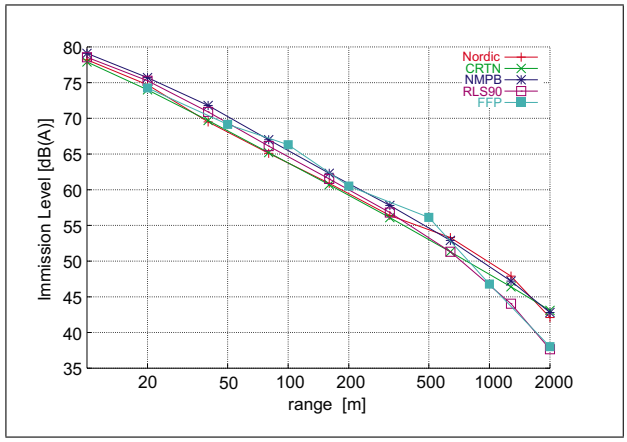

Figure 12. A-weighted sound pressure level of a long road as a function of distance to the receiver computed according to the European traffic noise guidelines NMPB-Routes, CRTN, Joint Nordic and RLS-90. Also shown is the result of an FFP-calculation for a stable atmosphere and a flow resistivity of $2.5{\cdot}10^5$ Pa s/m^2 for downwind propagation. This is the favourable condition for sound propagation mentioned e.g.in the German guideline.

flow rate of 1000 cars/hour, the percentage of heavy vehicles, trucks, etc. is set to zero and the speed limit to 100 km/h.

Also plotted in Figure 12 is the result of an FFP simulation for the meteorological conditions similar to those required in some of the guidelines. Wind and temperature profiles are typical for a stable atmosphere and the sound propagation direction is downwind from the road towards the receiver. The guidelines do not explicitly mention what ground impedance or flow resistivity of the ground enters into the predictions, but for grass land a flow resistivity of $2.5 \cdot 10^5$ Pa s/m^2 is a quite reasonable value for σ that has been used for this FFP calculation.

The large variation in wind speeds for the different neutral profiles listed in Table I could lead to the assumption of an equally large variation in the resulting sound pressure levels. However, as Figure 13 clearly shows, the different neutral wind profiles do not lead to significantly differing sound transmission losses for the downwind case.

The noise immissions computed for the neutrally stable profiles differ by not more than 2 dB(A) and they all show the same monotonic decrease with range. Therefore in the following all sound propagation calculations for the neutrally stable state were carried out with the profile labelled neutral-IV in Table I. A comparison with the result for stable wind and temperature profile leads to characteristic deviations in the sound pressure level at the receiver position especially in the intermediate range at about 500 m.

The influence of different meteorological conditions according to the weather classes on sound propagation over grass land are shown in Figure 14. Two groups of transmission loss curves are clearly separated: The upwind propagation results show a steeper slope i.e. large transmission losses regardless of the form of the profile. The same holds

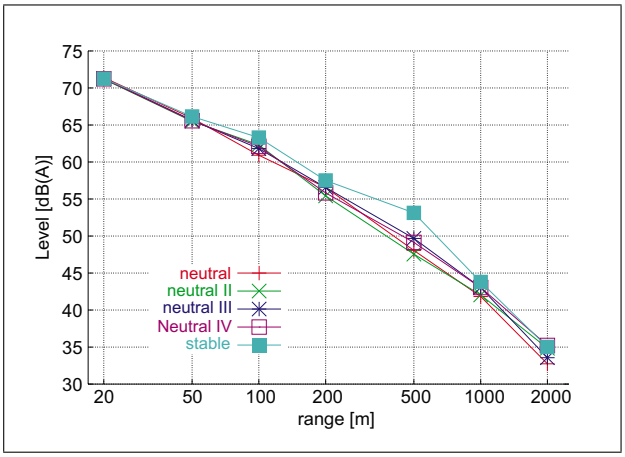

Figure 13. Comparison of A-weighted sound pressure level of a long straight road as a function of distance to the point of immission for different neutrally stable and one stable atmospheric profile. All computations were carried for a flow resistivity of $2.5 \cdot 10^5$ Pa s/m^2 and downwind propagation.

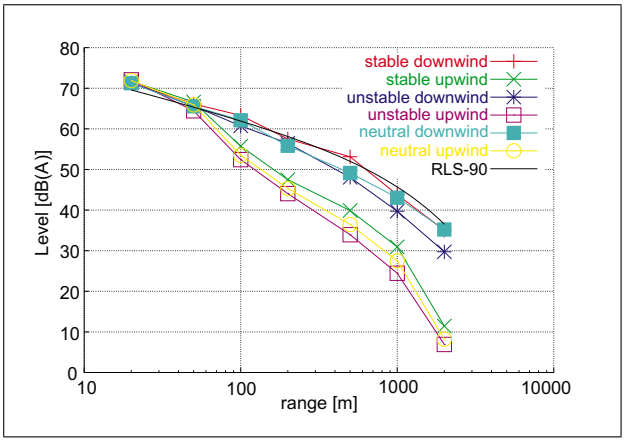

Figure 14. Noise Immissions (A-weighted sound pressure levels) of a long road as a function of distance to the receiver over grass land for stable, unstable and neutral wind and temperature stratifications. Sound propagation for downwind as well as upwind conditions is simulated. Also shown is the prediction of the German RLS-90 guideline.

for the three downwind cases for favourable propagation conditions.

Figure 15 makes it possible to separate the influence of wind and temperature profile for upwind, downwind and no wind conditions. The ground is modelled as the same porous medium with a flow resistivity of $2.5 \cdot 10^5$ Pa s/m^2 in all cases. There is a good agreement of the TL for downwind propagation with a stable wind and temperature profile with the prediction of the RLS-90 guideline for this favourable condition. The computation with the same wind profile but for a constant temperature of 10 °C is nearly indistinguishable from the mentioned uppermost curves. This clearly shows, that it is the wind profile that is responsible for the characteristic decay of sound pressure level with distance. For the upwind case the same holds true as the two lowermost curves show. The constant temperature calculation gives nearly an identical result compared to the full profile calculation. The curve with nearly constant slope of about −30 dB/decade is for the case of a homogenous atmosphere without any stratification. Of course this slope is not constant since all simulations include the effect of atmospheric absorption.

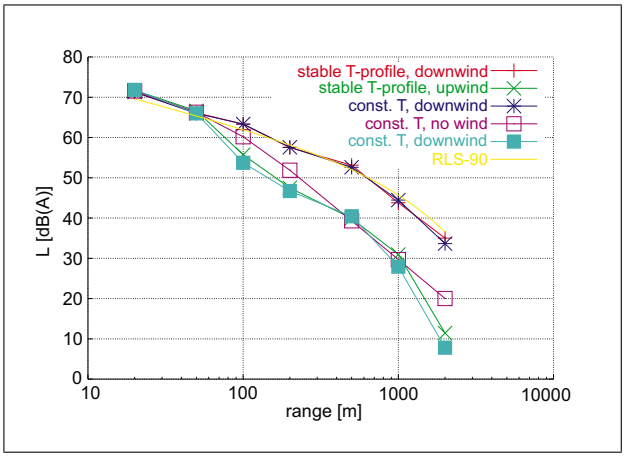

Figure 15. A-weighted sound pressure level of a long road as a function of distance to the receiver over grass land for downwind, upwind and no wind conditions with and without an additional temperature profile. Also shown is the prediction of the German RLS-90.

The computed sound levels from the FFP algorithm show a very good agreement with the German RLS-90 if the meteorological conditions assumed in the guideline are met. The slight downwind of not more than 3 m/s at a height of 10 m is modelled in the simulation with the help of Monin-Obhukov similarity theory. The stable temperature and wind profiles shown in Figure 9 and Figure 10 were used as input files for the FFP programme.

4. Conclusion

With general assumptions on source spectrum, power and geometry it is possible to compare the different guidelines and protocols to calculate traffic noise propagation. With the same hypothesis it is possible to calculate numerically the sound propagation for discrete frequencies and to integrate the results in order to get third-octave results. It is necessary to control the parameters for the numerical model thoroughly since assumptions about spectrum, geometry and spatial, incoherent wave superposition enter into the calculation. Adjusting the parameters of the different guidelines shows close similarity of the results.

These results are confirmed by the "exact" numerical simulation for downwind condition and propagation over medium-soft ground (grassland).

An advantage of the numerical model is to vary environmental parameters systematically and to study the result of changes in meteorology and ground impedance. The FFP is in particular suitable for the study of a layered medium including the ground impedance as complex boundary. It is

verified that the wind has the largest effect on noise propagation, provided realistic meteorological boundary-layer conditions are taken into account. The downwind assumption is very well justified as the most favourable propagation condition. If the noise propagates along an acoustically hard boundary, the sound pressure level is increased, which is not fully taken into account in the existing guidelines (if at all). The objective of the existing guidelines to provide a simple numerical scheme is very well met for a downwind condition and propagation over grassland and for medium distances (< 1 km).

Acknowledgement

This project was partialy funded by the EC (17224-2000-12 F1ED ISP DE). The authors thank the reviewers for their valuable comments.

References

[1] IMAGINE and Harmonoise www-homepage: Improved methods for the assessment of the generic impact of noise in the environment. www.imagine-project.org, 2008.

[2] E. M. Salomons: Building europe's future harmonized mapping methods. Acta Acustica united with Acustica **93** (2007) V–VI.

[3] D. Heimann, M. Bakermanns, J. Defrance, D. Kühner: Vertical sound speed profiles determined from meteorological measurements near ground. Acta Acustica united with Acustica **93** (2007) 228–240.

[4] J. Defrance et al.: Outdoor sound propagation reference model developed in the European Harmonoise project. Acta Acustica united with Acustica **93** (2007) 213–227.

[5] D. van Maercke, J. Defrance: Development of an analytical model for outdoor sound propagation within the Harmonoise project. Acta Acustica united with Acustica **93** (2007) 201–212.

[6] Immi. Wölfel Meßsysteme GmbH & Co. KG, www.woelfel.de.

[7] Cadna A. DataKustik GmbH, www.datakustik.de.

[8] IMAGINE and Harmonoise www-homepage. Delivery D14_WP2_HAR24-TR021018-TNO10. www.imagine-project.org, 2008.

[9] T. L. Richards, K. Attenborough: Accurate FFT-based Hankel-transforms for prediction of outdoor sound propagation. J. Sound Vib. **109** (1986) 157–167.

[10] S. Tooms, S. Taherzadeh, K. Attenborough: Sound propagation in a refracting fluid above a layered fluid-saturated porous elastic material. J. Acoust. Soc. Am. **93** (1993) 173–181.

[11] P. Chevret, P. Blanc-Benon, D. Juvé: A numerical model for sound propagation through a turbulent atmosphere near the ground. J. Acoust. Soc. Am. **100** (1996) 357–3599.

[12] Attenborough, Li, Horoshenko: Predicting outdoor sound. Taylor & Francis Ltd., 2006.

[13] B. Lihoreau, B. Gauvreau, M. Bérenier, P. Blanc-Benon, I. Calmet: Outdoor sound propagation modeling in realistic environments: Application of coupled parabolic and atmospheric models. J. Acoust. Soc. Am. **120** (2006) 110–119.

[14] K. Attenborough et al.: Benchmark cases for outdoor sound propagation models. J. Acoust. Soc. Amer. **97** (1995) 173–191.

[15] E. M. Salomons: Computational atmospheric acoustics. Kluwer Academic Publishers, Dordrecht, 2001.

[16] R. B. Stull: An introduction to boundary layer meteorology. Kluwer Academic Publishers, Dordrecht, 1989.